

# Building Tomograph – From Remote Sensing Data of Existing Buildings to Building Energy Simulation Input

Gorzalka, P.<sup>a</sup>; Estevam Schmiedt, J.<sup>b</sup>; Dahlke, D.<sup>c</sup>; Frommholz, D.<sup>c</sup>; Götttsche, J.<sup>d</sup>; Hoffschmidt, B.<sup>b</sup>; Israel, M.<sup>e</sup>; Linkiewicz, M.<sup>c</sup>; Patel, D.<sup>a</sup>; Plattner, S.<sup>e</sup>; Prahl, C.<sup>f</sup>; Schorn, C.<sup>d</sup>

<sup>a</sup> Institute of Solar Research at German Aerospace Center (DLR), Jülich, Germany

<sup>b</sup> Institute of Solar Research at German Aerospace Center (DLR), Cologne, Germany

<sup>c</sup> Institute of Optical Sensor Systems at German Aerospace Center (DLR), Berlin, Germany

<sup>d</sup> Solar-Institut Jülich (SIJ) at University of Applied Sciences Aachen (FH Aachen), Jülich, Germany

<sup>e</sup> Remote Sensing Technology Institute at German Aerospace Center (DLR), Oberpfaffenhofen, Germany

<sup>f</sup> Institute of Solar Research at German Aerospace Center (DLR), Tabernas, Spain

---

## Abstract

Existing buildings often have low energy efficiency standards. For the preparation of retrofits, reliable high-quality data about the status quo is required. However, state-of-the-art analysis methods mainly rely on on-site inspections by experts and hence tend to be cost-intensive. In addition, some of the necessary devices need to be installed inside the buildings. As a consequence, owners hesitate to obtain sufficient information about potential refurbishment measures for their houses and underestimate possible savings. Remote sensing measurement technologies have the potential to provide an easy-to-use and automatable way to energetically analyze existing buildings objectively. To prepare an energetic simulation of the status quo and of possible retrofit scenarios, remote sensing data from different data sources have to be merged and combined with additional knowledge about the building.

This contribution presents the current state of a project on the development of new and the optimization of conventional data acquisition methods for the energetic analysis of existing buildings solely based on contactless measurements, general information about the building, and data that residents can obtain with little effort. For the example of a single-family house in Morschenich, Germany, geometrical, semantical, and physical information are derived from photogrammetry and quantitative infrared measurements. Both are performed with the help of unmanned aerial vehicles (UAVs) and are compared to conventional methods for energy efficiency analysis regarding accuracy of and necessary effort for input data for building energy simulation. The concept of an object-oriented building model for measurement data processing is presented. Furthermore, an outlook is given on the project involving advanced remote sensing techniques such as ultrasound and microwave radar application for the measurement of additional energetic building parameters.

*Keywords:* building tomograph; remote sensing; building physics; energy performance; thermography; infrared; building models; three-dimensional

---

## 1. Introduction

Energy efficiency improvements on existing buildings have the potential to both decrease greenhouse gas emissions related to housing and to be economically beneficial for building owners and/or residents. However, refurbishment measures reducing the energy consumption are not carried out as widely as they should be. One reason for this gap is that many owners do not know about the potential savings that can be realized on their buildings [1]. They do not feel the need to invest the cost and effort involved with the on-site measurements which are necessary to obtain the information needed to determine optimal refurbishment solutions for their individual cases.

The work presented is part of an ongoing research project called “building tomograph” run by the German Aerospace Center (DLR) and Solar-Institut Jülich (SIJ) at the University of Applied Sciences Aachen that intends to make remote sensing technologies applicable for energetic analyses of buildings [2]. Its goal is to develop a tool box of measurement and analysis methods to determine the energetically relevant properties of existing building envelopes quickly and accurately. Thus, single buildings or whole districts may be examined in short time to obtain crucial information for the development of refurbishment strategies or about loads of the energy distribution networks. A reference building provides a validated test ground for remote sensing campaigns and to assess the

suitability and accuracy of the techniques used in the project. The structure itself is located in the German village of Morschenich, North Rhine-Westphalia. It provides free accessibility from all directions, typical wall structures, and the possibility to let unmanned aerial vehicles (UAVs) fly around the building without obstacles. As the house is unoccupied and will be dismantled, extensive sample taking and deconstruction of construction elements is possible.

In this paper, the current state of the research project is summarized. For this purpose the results of actual measurements and a set of photogrammetric data products with regard to the reference building are presented in a sequence of dedicated sections. Following this introduction, section 2 presents reference measurements using conventional methods. The section also provides an insight into the state of the art and the necessary effort to obtain reference values for the structure. Section 3 outlines the suggested remote sensing workflow for analyzing the energetic properties of the building. The sections 4 to 6 provide a detailed description of how remote sensing methods have been used up until now within the project's time frame by elaborating on UAV-based image acquisition and preprocessing (section 4), photogrammetric building reconstruction (section 5), and quantitative infrared thermography (section 6). In section 7, the data processing approach is presented which is developed to merge the remote sensing data from different sources, generating energetic simulation input parameters. Section 8 concludes the paper with a summary of the results obtained so far as well as an outlook to future work.

## 2. Energetic building assessment with conventional methods to obtain reference data

At the current state of the art, several methods are in use to obtain input data for the energetic assessment of buildings. They cover various aspects of energy consumption and heat demand and are useful to identify different types of building weaknesses. When combined, conventional analysis methods can provide the currently most reliable evaluation of the complete building. In order to examine the energetic quality of the building envelope, terrestrial laser scanning, the blower door test, infrared thermography, and U-value determination are widely used. With ground-based laser scanners the object's inside and outside surfaces are spatially sampled by an invisible concentrated light beam in a selectable resolution and quality. As a result, the building geometry gets represented by a dense three-dimensional point cloud. The blower door test allows for the determination of the air exchange rate and the detection of possible leaks in the building hull. It pressurizes or depressurizes the interior of the structure using a unidirectional fan and monitors the air flow necessary to hold the pressure difference over time. Standard infrared thermography provides qualitative information about the insulation and possible weak points, such as thermal bridges. If accurate plans of the building exist, U-values are usually calculated on the basis of wall structure, material data, and layer thicknesses. If no up-to-date plans are available (as it is the case for many existing buildings), U-values are guessed using typologies or based on the experience of an expert. They can also be measured by taking material samples from the site. In exceptional cases, U-values are determined directly through on-wall measurements.

The advantages of these approaches are that they are well-known, widely recognized by the community and relatively accurate with respect to the energetic assessment of a building under well-defined conditions. Their results are used to prepare energetic assessment reports – sometimes including dynamic simulations –, energy performance certificates, and the recommendation of optimization measures. However, depending on the desired level of detail the state-of-the-art methods are time-consuming and require special devices and instruments with specific software solutions making them impractical and rather pricey.

The following paragraph describes the workflow for energetic building assessment applied to the reference building. This comprises data acquisition, experimental setup, and energetic simulation. Afterwards, an overview of the results of the analysis is given.

### *Application of conventional data acquisition methods to the reference building*

A series of measurements on the reference building was performed in Spring 2018. On the basis of a 3D point cloud derived from indoor and outdoor laser scans, the building was reconstructed using the software Revit Autodesk. With the help of the OpenStudio plugin for the SketchUp 3D tool from Google, information on the wall structure, materials, and physical data derived from samples as well as the relationship of building surfaces to their environment were introduced into the model. Afterwards, it was transferred to the simulation software EnergyPlus as a gbXML file. Data on the air exchange rate (from a blower door test) and on thermal bridges (estimated based on

qualitative infrared thermography) as well as estimated values for the sky temperature (calculated in relation to the dry bulb temperature) and soil temperature (based on the measured temperatures in the unheated basement and recorded data of a meteorological station in the North of North Rhine-Westphalia) were added. The general workflow for the determination of an energetic assessment of the reference building including the energetic simulation is shown in Figure 1.

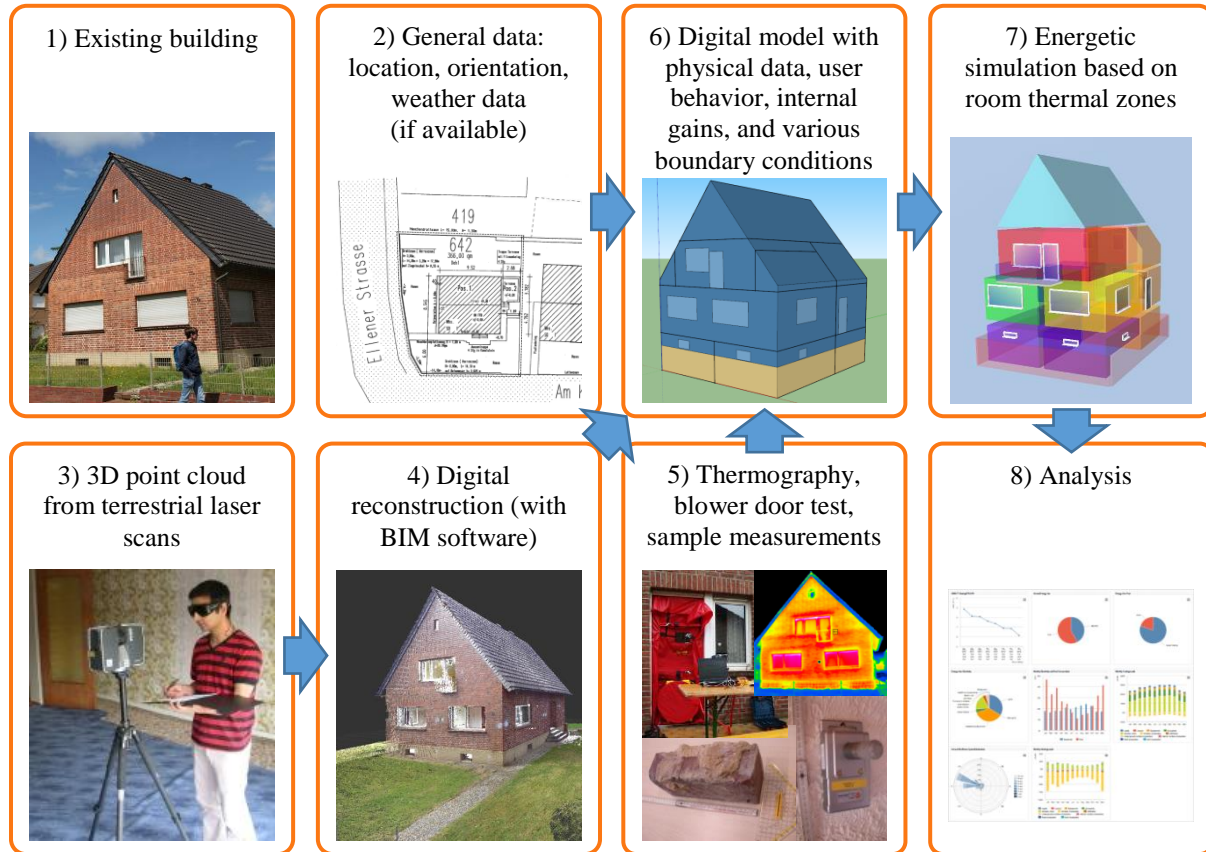


Figure 1: Workflow for conventional energetic building assessment

*Experimental setup: Heating and temperature measurements*

As it is going to be demolished, the reference building neither was heated nor is its space heating system currently operable. During a measurement campaign in Spring 2018, the first floor was heated by a portable 9 kW fan heater. On the second floor, each room was equipped with a single electric heater with a power of 2 kW, 2 kW, and 1.2 kW respectively. All devices were set up to work at the highest level delivering as much heat as specified on the rating plate. The attic space and the basement were not heated. Energy consumption was recorded periodically through manual read-out of a Ferraris-type electric meter. Room temperature in the basement and on the first and second floor got recorded automatically as were the outside wall surface and ambient temperatures. The mean temperature of the building was calculated from the measured room temperatures on the two upper floors using volume-based weighting. The general arrangement of the electric heaters and the spots where the main temperature measurements took place are shown in Figure 2.

*Energetic simulation: Input data*

In order to validate the building model with its assumptions and physical parameters, mean building temperature, basement temperature, energy consumption, and surface temperatures during the measurement campaign were simulated using EnergyPlus. For this reason, a weather data file was created containing the ambient temperature at Morschenich during the campaign as well as wind velocity, wind direction, and radiation values from a weather station in Jülich (in a distance of about 15 km) for the corresponding time interval. Weather data preceding the start

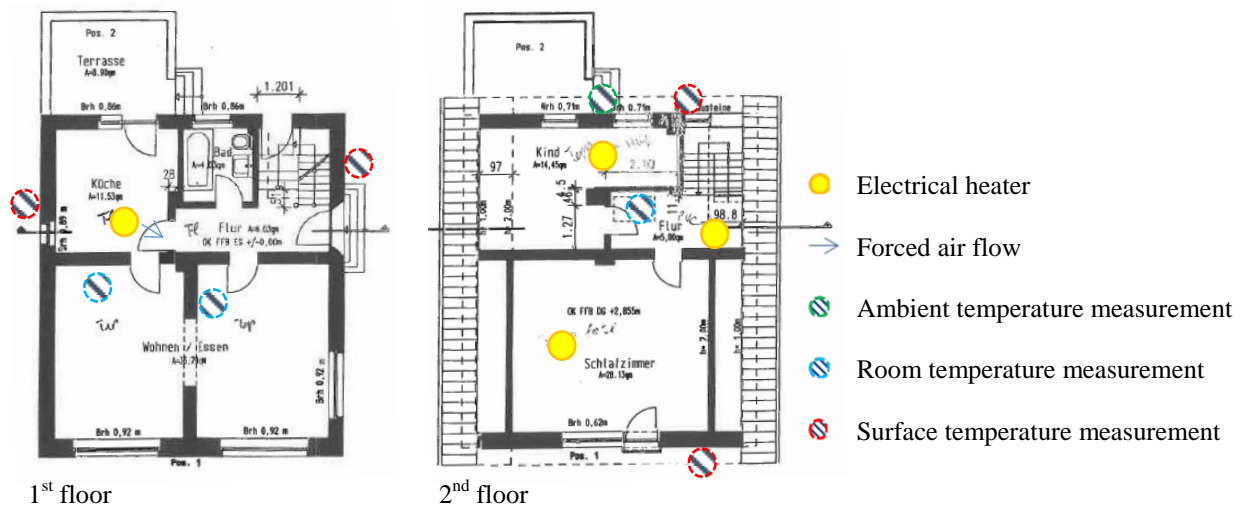


Figure 2: Ground plan of first and second floor of the reference building with main measurement points and heating setup

of the measurements was modified in order to guarantee the same range of initial temperatures during simulation compared to reality.

In the simulation, every room is treated as a thermal zone. As on the first floor only one electric heater was installed, the simulation heating load was distributed to the thermal zones proportionally to their floor area. Maximum heating power during simulation was adjusted to 71 % of the peak load because unexpectedly low electric meter values lead to the conclusion that the heaters stopped operating from time to time, probably due to local overheating at their thermostat. Consequently, the thermostat set points could not be used as heating set points for simulation. Instead, the simulation heating set points were modified to make the simulated energy consumption match the actual one for every interval between the electric meter read-outs, but complying with the maximum value of 38.5°C. The attic spaces and the basement are treated as unheated. For the simulation of the basement temperature an additional simulation had to be carried out in order to adjust the basement surface temperature towards the soil.

*Energetic simulation: Validation of the model*

In order to verify the model parameters, three sources of data were available: room temperatures, energy consumption, and outside surface temperatures. First results show a good agreement of the simulated and measured values. In the following, they are presented in detail.

Figure 3 shows simulated and measured values of mean building temperature, basement temperature, and cumulated energy consumption over time. The measurement campaign starts with powering up the heating system. The peak in the basement temperature measured in the beginning is due to an initial time delay of the respective temperature sensor and hence can be ignored. The negative/positive temperature peaks on April 12 occur because of a blower door test on that day. Simulated values for the basement are very close to the measured temperatures; the deviation remains less than the specified accuracy of ±0.5 K of the installed sensor (shown as gray intervals in Figure 3). Simulated mean building temperatures largely match the measured values. Even the dynamic effect of the blower door test can be reproduced approximately by assuming the actual air exchange rate on that particular day.

Although it was also used for adjusting the heating set points and therefore to some extent is a simulation input parameter, the energy consumption of the heating system is a second source for verification of the simulation model. In Figure 3, it can be seen that the simulated curve is approximately congruent with the measured curve. The difference in total energy consumption might be explained by the inhomogeneous distribution of the heat within the house which cannot be fully compensated by just mixing the air with a fan. In contrast to this, in the simulation model, every room is considered a homogeneous zone with its specific surfaces, physics, and a static electric heating power. Moreover, a constant infiltration rate was assumed during the EnergyPlus simulation run while at the end of

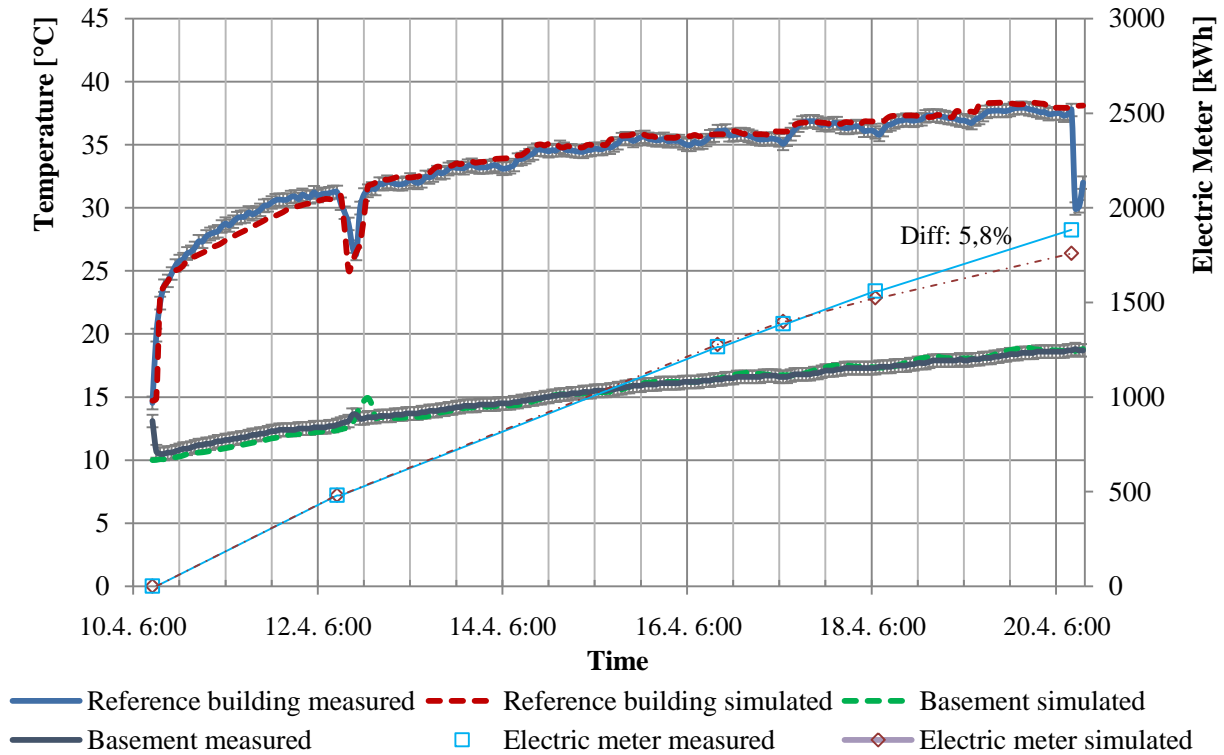


Figure 3: Simulated and measured values for mean building temperature, basement temperature, and cumulated energy consumption over the time of the reference measurement

the measurement campaign slightly higher wind velocities were recorded. The cooling phase was not examined because immediately after finishing the heating phase another blower door test took place.

Wall surface temperatures were measured and simulated. Figure 4 shows the results for a cloudless day during the campaign. As the whole building is orientated approximately 25° counterclockwise from true north, the cardinal directions specified do not represent the wall orientations exactly. The surface temperature of the east wall rises at first in the morning when it gets hit by the solar radiation with a low incidence angle towards the wall. Shortly afterwards, the south wall surface temperature increases due to the slight south-eastern orientation. The temperature of the west wall shows the highest absolute values because the angle of incidence is advantageous for a long period of time in the afternoon. On top of that, the high temperatures on the west surface are supported by the rising ambient air and inside temperatures during the day. The reason for the fact that the simulated values for the west wall rise earlier than the measured values is the placement of the surface temperature sensor next to the north/west corner of the building. The north face eventually shows a small peak when the solar radiation partially hits the wall surface during the end of the day.

In any case small deviations between the measured and simulated samples can be explained by having used radiation data from a weather station nearby. Moreover, effects from shadow cast by the roof overhangs were neglected during the simulation. Considering that each temperature measurement was taken at a certain specific point and that the simulation data comprises the calculated mean surface temperatures of the respective thermal zones, the simulation shows a good approximation of the measured surface temperatures for all four cardinal directions.

*Conclusion on the reference model*

As a conclusion, it can be stated that the EnergyPlus model derived from the actually measured values has been successfully validated and may serve as a basis for a future comparison with the remote sensing approach under development as a part of the project. In Table 1, the most relevant building analysis results and simulation parameters are listed together with a reference to their source. Acquiring the necessary parameters required a substantial amount of manual effort and heavily relied on (reasonable) assumptions and literature values.

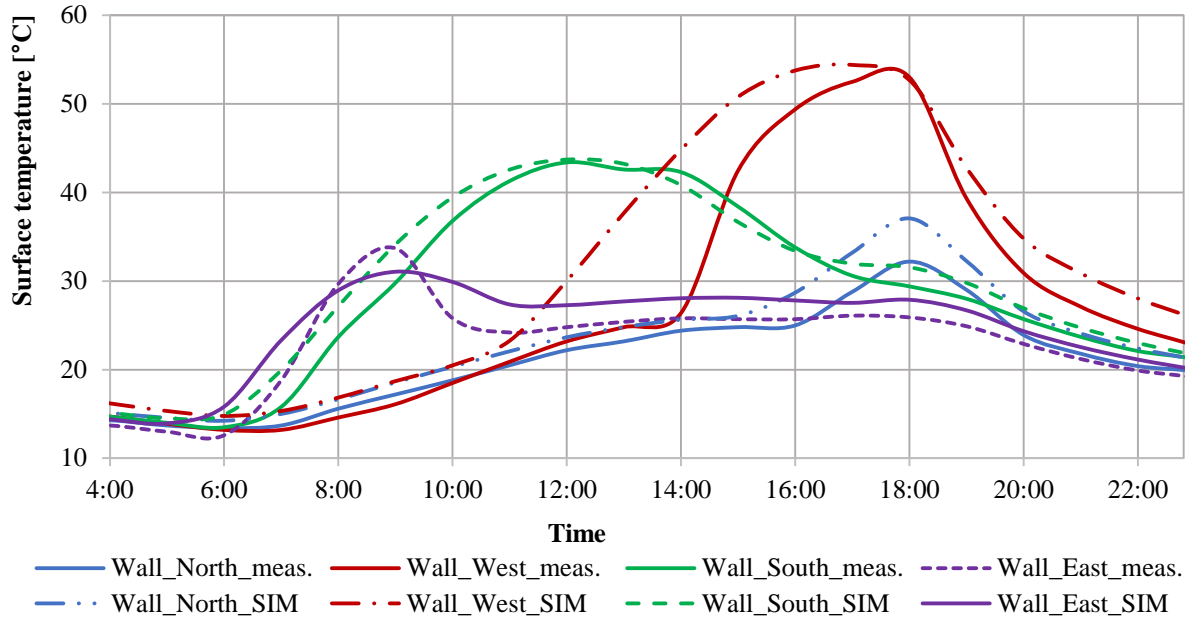


Figure 4: Measured and simulated wall surface temperatures for different geographical directions on a cloudless day (18/4/2018)

Table 1: Overview of the most relevant simulation parameters

Parameter	Value	Unit	Reference
<b>Orientation (counterclockwise from true north)</b>	25	°	Google Earth
<b>Heated zone</b>	7	rooms	defined
<b>Unheated zone</b>	4 basement rooms 3 attic spaces	[-]	defined
<b>Infiltration rate (continuous)</b>	0.225 <sup>1</sup>	1/h	Measurement, calculation
<b>Thermal bridges (complete building envelope)</b>	0.1	W/(m <sup>2</sup> K)	Assumption based on IR
<b>Soil temperature</b>	14.0	°C	Assumption based on IR and meteorological station
<b>U-value walls</b>	1.095 – 1.95	W/(m <sup>2</sup> K)	Based on literature values
<b>U-value roof (insulated)</b>	0.418	W/(m <sup>2</sup> K)	Based on literature values
<b>U-value roof (without insulation)</b>	6.85	W/(m <sup>2</sup> K)	Based on literature values
<b>Surface convection R<sub>i</sub> and R<sub>a</sub></b>	various	m <sup>2</sup> K/W	calculated <sup>2</sup>
<b>U-value Windows</b>	2.22 – 2.60	W/(m <sup>2</sup> K)	Based on literature values
<b>U-value floor</b>	2.34	W/(m <sup>2</sup> K)	Based on literature values
<b>U-value ceiling towards attic space</b>	0.423	W/(m <sup>2</sup> K)	Based on literature values
<b>Shading</b>	none	[-]	Not specified
<b>Density: brick / pumice stone / concrete</b>	1800 / 1200 / 2400	kg/m <sup>3</sup>	Literature values
<b>Conductivity: brick / pumice stone / concrete</b>	1.05 / 0.58 / 2.1	W/(mK)	Literature values
<b>Specific heat: brick / pumice stone / concrete</b>	836 / 800 / 1000	J/(kgK)	Literature values
<b>Solar absorptance complete building envelope</b>	0.7	[-]	Assumption based on verification of wall temperatures
<b>Maximum heating power (total building)</b>	10.1	kW	Measurement
<b>People, lights, additional internal gains</b>	none	[-]	Not specified

<sup>1</sup> Calculated at 1...2 Pa pressure difference based on the measured low wind velocity during measurement campaign

<sup>2</sup> R<sub>i</sub> inside correlation from models developed by [3, 4], R<sub>a</sub> outside correlation from models developed by [3–5]

### 3. Suggested workflow for the energetic assessment of buildings using remote sensing

Remote sensing technologies have the potential to reduce the effort necessary for the energetic assessment of buildings if it can be managed to at least partially substitute the laborious on-site inspections involving the conventional methods mentioned above. Thus, the goal of the ongoing research project “building tomograph” is to develop an appropriate remote sensing methodology and to estimate the accuracy that can be achieved with the technologies identified. In this section, a combination of sensors for the energetic analysis of buildings is proposed. A comparison of the conventional analysis and the proposed approach is listed in Table 2.

**Table 2: Comparison of different data sources for conventional analysis and those used for the “building tomograph” project**

Information	Conventional analysis	Building tomograph
<b>3D point cloud</b>	Laser scans with RGB camera for coloring	Photogrammetry based on UAV aerial RGB imagery
<b>Envelope surface geometry</b>	Autodesk Recap (with manual input)	Automatic identification of surfaces and semantics
<b>Inside geometry</b>	Laser scans for each room, Autodesk Recap	Story height estimation from window position or similar story-related features
<b>Location and orientation</b>	Google Earth	GPS-tagged images
<b>Roof and wall U-values</b>	Calculation based on literature values	Sensor fusion of quantitative infrared, microwave radar, literature values
<b>Thermal bridges</b>	Assumption based on IR	Estimation based on IR
<b>Air infiltration</b>	Blower door test	Ultrasound measurement
<b>Shading</b>	Not specified	Polygon clipping on CityGML objects

Since they can be positioned freely within the space around a building, UAVs provide a flexible platform for image acquisition. They allow capturing close-range aerial imagery which subsequently can be used for high-resolution photogrammetric building reconstruction. The involved devices are handier and less expensive than a terrestrial laser scanner. Furthermore, it becomes possible and more convenient to picture details of the building façade or roof that are not visible from any possible laser scanner position on the ground. Taking oriented images and pre-processing can be easily carried out with the latest advances in photogrammetric software tools although manual input is still needed as described in section 4. The same holds for the reconstruction process (section 5) generating polygonal building hulls with semantic annotations which, in contrast to bare point clouds, are the representation most state-of-the-art 3D tools are expecting as an input.

To obtain the interior geometry of a structure, additional information is needed which of course cannot be obtained by remote sensing from the outside. Assumptions on the inside layout can be made from the story heights derived for example from window positions. However, interior walls will not get modelled this way. For future applications it may hence be advantageous to include floor plan recognition algorithms based on existing printed plans [6] or smartphone imagery [7].

Thermal infrared (TIR) imagery is a state-of-the-art technology for a qualitative analysis of the thermal quality of the building envelope. Utilizing UAVs, it is possible to obtain high-quality infrared images of the structure from different perspectives. This does not only allow for 3D infrared visualization and to identify thermal bridges, but may also help to approximately quantify the U-values of wall and roof surfaces. A possible approach on how to achieve this goal is presented in section 6. However, in order to determine the heat flow through the walls, the infrared images must be taken when sunlight is not present yet since its absorption will distort the measured values. As a consequence, there is only a short time frame before actual sunrise during which it is feasible to obtain both IR and standard RGB imagery during a single flight. Even if quantification of the U-values cannot be realized accurately enough, regions with different building material layer structures can be identified. For a detailed wall structure analysis of these regions, a promising approach involving non-destructive testing is the use of microwave radar [8, 9]. The technology is under development at DLR and will be tested on the reference building in 2019.

Another important value for energetic building assessment is the air infiltration rate. The state-of-the-art method to determine this value is the blower door test explained previously. It tends to be expensive, laborious, and time-consuming. To overcome this, research on an approach using ultrasound technologies is currently conducted [10].

#### 4. UAV-bound image acquisition and pre-processing

In order to create a three-dimensional model of the reference building, a large set of more than 1000 GPS-tagged and hence roughly oriented RGB images was captured by a standard digital single-lens reflex camera (18 megapixels) mounted on a UAV. For reconstruction of the building geometry, nadir-looking and oblique images were acquired during a pre-planned flight finished automatically within a few minutes. To capture even small details of the façades, close-range images with a nearly horizontal orientation were recorded by manually operating the involved hexacopter in a distance of 5 m to the building in different altitudes. However, this time-consuming step which cannot be performed automatically yet and thus has to be carried out by an experienced drone pilot is only necessary if a close-range examination of possible façade damages is required and is not needed for only deriving a generalized 3D-model like a CityGML representation of the building.

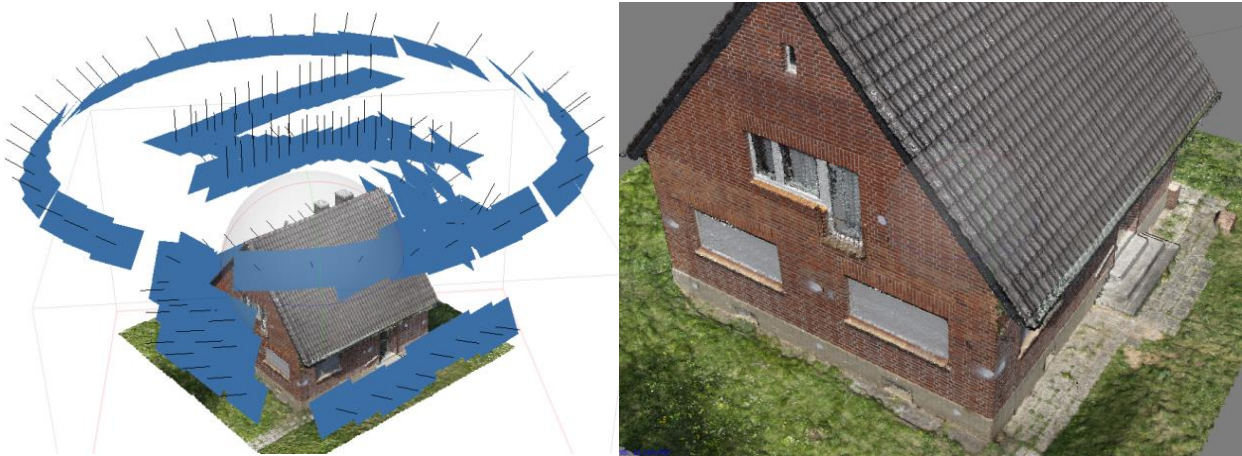


**Figure 5: Camera positions for the selected subset of nadir, oblique and near-horizontal images as calculated by Agisoft Photoscan (left), 3D point cloud with very high detail (approx. 12 million points, right)**

From the stock of images a subset of 152 GPS-tagged images with sufficient overlap ( $> 60\%$ ) was selected manually and processed with the commercial software tool Agisoft PhotoScan. After automatically detecting and matching tie points inside the images their orientation which originates from the GPS receiver of the drone gets refined resulting in an accurate estimate for the global camera position and rotation at the time of exposure. In Figure 5 (left), camera positions and orientations for the selected subset of images are depicted. From this set of oriented images a 3D point cloud with approximately 12 million points (Figure 5 (right)) was calculated by the software, providing a spatial resolution of less than 1 cm. This point cloud can now serve as an input to generate the polygonal building hull with semantic annotations useful for building information systems or subsequent energy simulation.

Since due to its rotors the UAV used cannot take upward-looking images the point cloud resulting from UAV flights lacks information under the roof overhangs and canopies of the building. This obviously is a disadvantage compared to point clouds derived from a terrestrial laser scanner. An example for this difference can be seen in Figure 6. However, ground-based laser scans expose visibility problems when regions behind balconies and roof installations. With some modifications applied to the UAV flight control it will probably be possible to cover the missing regions in the near future as well.



**Figure 6: Blind spaces below roof overhangs and canopies in photogrammetry-based point cloud (left) and the respective regions in laser scanner point cloud (middle, right)**

In addition to the acquisition of images in the visible range of the spectrum, a TIR camera was also carried by the UAV in order to measure the temperature of the building surfaces. In comparison to the RGB images the spatial resolution of the TIR camera is significantly lower (640x512 pixels). However, the high-resolution RGB data can be superimposed with the thermal imagery to better interpret relevant features. Section 6 discusses infrared thermography using drones in detail.

Furthermore, a UAV-borne hyperspectral camera (Cubert UHD-185) was used to derive information about the surface materials of the building components as an additional input to the building analysis. It was shown previously that, using an aircraft-borne hyperspectral sensor, the detection of different roof materials (concrete, zinc, aluminum, copper, plastic polymers) is generally possible [11]. In further work, the suitability of the rather low-resolution 50x50 pixel UAV sensor for this task will be examined.

## 5. Photogrammetric building reconstruction

In order to derive a polygonal 3D model of the sample building with semantic annotations, the point cloud from Agisoft PhotoScan was used. In a first step, it was converted into a digital surface model<sup>3</sup> (DSM, depicted in Figure 7a) which effectively encodes the elevation of the scene. Also, having the DSM, a digital terrain model<sup>3</sup> (DTM) was obtained providing an estimate for the ground height around the building by repeatedly shifting windows of varying size over the height bitmap [12]. In the following, the workflow for the photogrammetric building reconstruction is summarized. A detailed description is available in previous publications of the authors of this paper [13–15].

### *Façade and roof modelling*

To model the wall surfaces of the structure, the 3D point cloud gets projected into the xy plane subdivided by a regular grid. The spatial distribution and z histogram is analyzed for façade pieces which are approximated by line segments using RANSAC [16]. Adjacent line segments again undergo linear regression when their directional difference is below a fixed angular threshold. The resulting façade fragments will be intersected if their endpoints are locally adjacent within the grid forming a closed two-dimensional contour. The step from line segments to façade fragments is shown in Figure 7b for the reference building.

For the extraction of roof planes, slope and aspect of the DSM pixels within the area enclosed by the wall surfaces are computed and similar pixels are grouped. During this process chimneys and other installations on the top get identified and eliminated for now. Any resulting gaps between or inside the roof segments are filled by breath-first

<sup>3</sup> DSM represents earth surface including any objects on it, DTM only represents the natural terrain's elevation

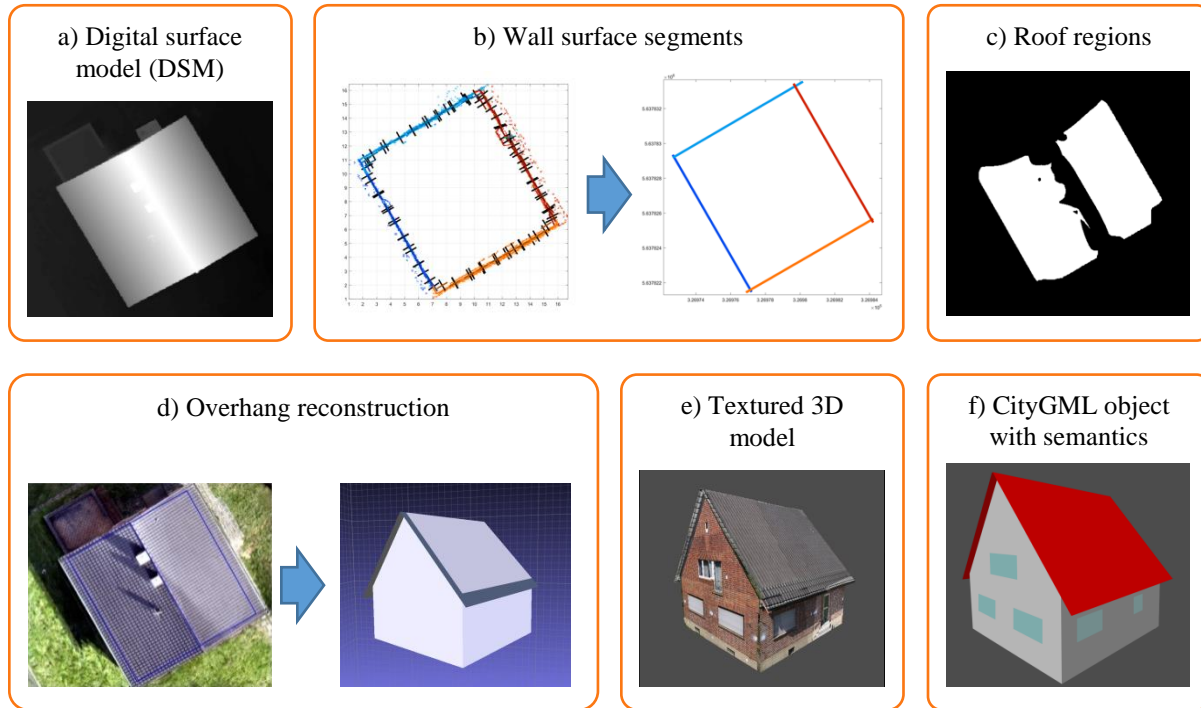


Figure 7: Photogrammetric building reconstruction stages

region growing yielding closed surfaces (see Figure 7c). The surfaces are then geometrically combined with the wall contours that for this purpose get perpendicularly erected to match the ground height from the DTM. The outcome of this process is a preliminary building hull with known surface semantics (for example roof or wall surface) according to its construction.

#### *Roof overhangs*

In western architecture, roofs often come with overhangs which, if not modeled, will disturb texture mapping and façade element classification. Since they cast shadows, energetic simulations on the building are influenced, too. To extract the eaves, the polygonal outline given by the wall surfaces of a building is projected onto the DSM of the scene (see Figure 7d). The roof edges are then moved along their normal vectors with subpixel accuracy up to the end of the roof overhangs which are represented by the zero-crossings of the second-order derivative of the height map in the gradient direction. The previously reconstructed roof polygons of the building model then get extended accordingly.

#### *Texture mapping*

For realistic renderings of the reconstructed building its naked hull is textured directly from the available input images. Each model polygon gets assigned to a sorted list of oriented source bitmaps depending on the effective resolution on the respective 3D surface. Following a complex visibility test to bypass any occluders and a tree-based coverage analysis the remaining image candidates are written to a single space-optimized texture atlas with minimal resampling. Perspective correction relative to the camera position is performed before both the atlas and texture coordinates eventually are added to the model.

#### *Window extraction and reintegration*

Having the texture atlas, windows can be directly extracted from its unrectified polygonal texture patches. However, since rectification allows geometrical features to be exploited, an orthogonal projection is computed per building polygon to undistort the wall surfaces before classification. Subsequently, openings are detected by iteratively scanning the transformed texture patches horizontally for stories and for façade elements per level. To identify openings and windows, brightness differences and an orthogonality criterion are evaluated. The elements found get vectorized and reintegrated into the building hull by sparsely ray-tracing their vertices starting at the corresponding

camera position. The final geometry is stored in the open Alias/Wavefront OBJ format for visualization and as CityGML objects for GIS applications with the semantics collected during the reconstruction process (see Figure 7e and f).

*Evaluation on test building*

For the photogrammetric reconstruction of the test building, the chosen set of 152 JPEG images recorded by the UAV pictures the building from various positions with a resolution of approximately 3 cm/pixel. Using the process described in the previous paragraphs a polygonal 3D reconstruction of the hull of the structure was created. Comparing the resulting surfaces against the point cloud revealed a positional deviation of 5 cm on average for 99 % of all vertices and 6 cm for all 3D samples including those that belong to any displaced rooftop installations.

**6. Quantitative infrared thermography using UAVs**

In recent time, infrared thermography (IRT) is being tested to measure the heat transfer coefficient (U-value) of building walls. IRT from inside a building has provided acceptable outcomes [17, 18]. For the reference building, our approach for the external IRT measurement with an infrared camera carried by a UAV was used [19]. In this work, it is summarized and its application to the reference building is described.

*Approach for external U-value measurement by infrared thermography for building walls*

The U-value of an outer building wall can be defined as described by equation (1). In steady state it is equal to the heat per time and area passing through the wall divided by the difference of indoor and outdoor air temperature.

$$\begin{aligned}
 U &= \frac{\dot{q}}{T_{in,air} - T_{out,air}} = \frac{\dot{q}_{rad} + \dot{q}_{conv}}{T_{in,air} - T_{out,air}} \\
 &= \frac{\epsilon_{wall} \cdot \sigma \cdot (T_{wall}^4 - T_{reflected,outside}^4) + h_{c,outside} \cdot (T_{wall} - T_{out,air})}{T_{in,air} - T_{out,air}}
 \end{aligned}
 \tag{1}$$

Here,  $U$  denotes the heat transfer coefficient. The variable  $\dot{q}$  stands for the specific heat flux through the wall. In a steady state it is equal to the sum of the specific heat flux emitted from the wall by radiation  $\dot{q}_{rad}$  and by convection  $\dot{q}_{conv}$ .  $T_{in,air}$  is the air temperature near the wall from inside the building, and  $T_{out,air}$  represents the outdoor air temperature near the wall. In the second part of the equation, the radiative portion is expressed by the thermal emissivity of the outside wall surface  $\epsilon_{wall}$ , the Stefan-Boltzmann constant  $\sigma$ , an averaged outside reflected ambient temperature  $T_{reflected,outside}$ , and the surface temperature of the wall  $T_{wall}$ . For the convective part,  $h_{c,outside}$  is the convective heat transfer coefficient on the outside of the wall.

**Table 3: Parameters required for measuring U-value using IRT**

Parameters	Sensors
<b>Emissivity</b>	Reference table
<b>Radiation coming from test object</b>	IR camera
<b>Ambient reflected temperature</b>	IR camera
<b>Outside air temperature</b>	Temperature sensor (NiCr-Ni)
<b>Inside air temperature</b>	Temperature sensor (NiCr-Ni)
<b>Wind velocity</b>	Vane anemometer

In Table 3 all parameters used for calculating the U-value are listed together with the corresponding sensors. To measure the U-value using a UAV-mounted TIR camera with our approach, the wall surface temperature is not calculated. Instead, the radiation coming from the wall surface  $W$  is determined and used to calculate the U-value. With the assumption that the object’s surface behaves like an opaque grey body without spectral and directional variations in emissivity,  $W$  can be inserted into equation (1) which gives

$$U = \frac{\overbrace{W - \sigma \cdot T_{reflected,outside}^4}^{\text{radiative term}} + \overbrace{h_{c,outside} \cdot \sqrt[4]{\frac{W - (1 - \epsilon_{wall}) \cdot \sigma \cdot T_{reflected,outside}^4}{\epsilon_{wall} \cdot \sigma}} - T_{out,air}}^{\text{convective term}}}{T_{in,air} - T_{out,air}} \quad (2)$$

An uncertainty analysis was carried out using this approach. As a result, emissivity and indoor air temperature only have a very small influence on the U-value measurement given a high temperature difference between inside and outside. Therefore, the emissivity value can be taken from emissivity tables and using an inside air temperature sensor is not strictly necessary. [19]

*U-Value measurement on reference building*

The measurement campaign took place at the reference building in Morschenich in April 2018 between 5 am and 6 am. The primary reason to choose this time was to avoid solar radiation and obtain a large temperature difference. A FLIR Duo Pro R (microbolometer detector) thermal camera was used to measure quantities like radiation coming from the wall surface and the reflected radiation (using crumpled aluminum foil).

A close qualitative observation of the thermal image of the north wall (Figure 8) exposes some interesting results. For example, the areas above both the windows seem to have higher temperature, probably meaning less insulation, whereas the areas next to both windows are insulating better. A detailed inspection from the inside of the building by removing the plaster layer off the wall led to the result that, while the outer layer of the wall is completely made of brick, in the area above the window the inner layer consists of reinforced concrete. The rest of the inner layer is built out of pumice stone. The use of different materials here explains partly the difference in temperature distribution because pumice stone insulates better than concrete. The reason for the rest of the temperature differences still has to be investigated.

A reference measurement of the U-value was carried out with the Heat Flux Meter (HFM) method as described in ISO 9869-1 [20]. The U-value measured with the HFM method is 1.24 W/(m²K) as an averaged value over the seven consecutive days of the measurement period.

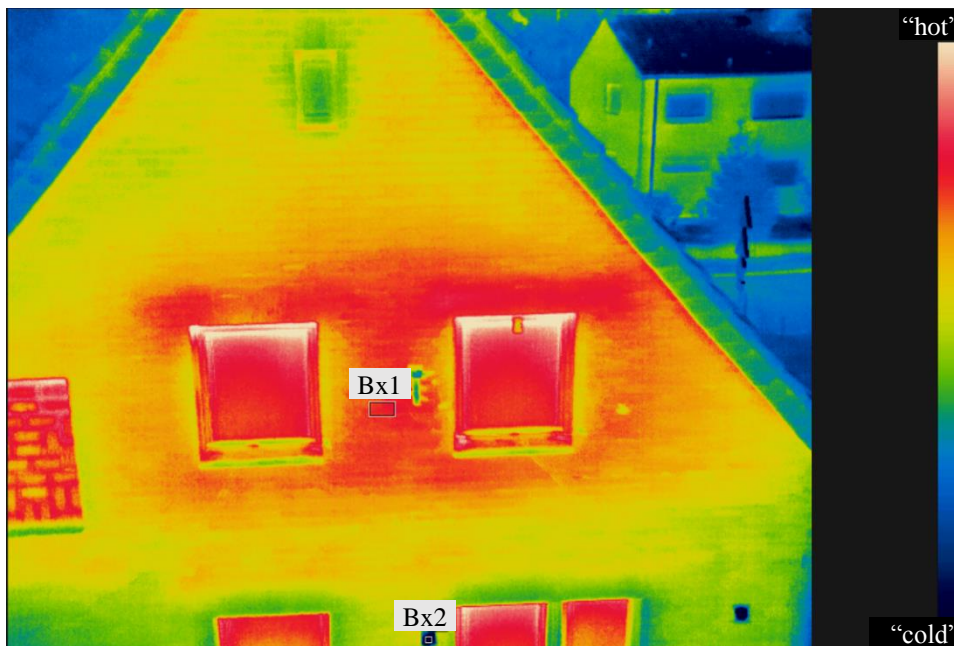


Figure 8: IR image of north wall showing area for U-value measurement (Bx1) and for reflected temperature on crumpled aluminum foil (Bx2)

In Figure 8, area Bx1 is used to measure the radiation coming from the wall while Bx2 is used for the reflected temperature measurement. Bx1 was selected because the heat flux sensors used for the reference HFM method were also mounted in this area from the inside. The evaluation of the IRT measurements to determine U-values is still ongoing, but some valuable insights of data evaluation are described in the following.

Due to the use of different materials in a single wall the usage of an average temperature for a whole façade to calculate its U-value is not possible. One approach is to select a small area of the whole wall (like Bx1 in Figure 8) and then to measure the U-value there. In this manner, the U-value result is valid only for that small area and not for the whole wall. Hence, it normally is impossible to make any assumptions about the insulation quality of the entire wall. However, if certain regions of the image of the wall are considered representative, this approach is favorable.

Another way is shown in Figure 9. Multiple areas are selected for U-value calculation. By doing this, the insulation property of the wall can be analyzed locally and refurbishment measures can be recommended effectively. Regions can be as large as desired as long as the surface temperature is nearly constant. An area-weighted average can be used to determine the U-value for a complete façade.

It will be interesting to see which approach provides acceptable results for the U-value calculation. In a first evaluation, the data analysis process has provided much higher U-values than the HFM results. This deviation is being studied in more detail. Moreover, there are more open topics to be worked on like angle dependency, selection of time for the IRT measurement, convective heat transfer effects on the TIR camera temperature (housing and core) during the measurement and the influence of dynamic effects on U-value calculation.

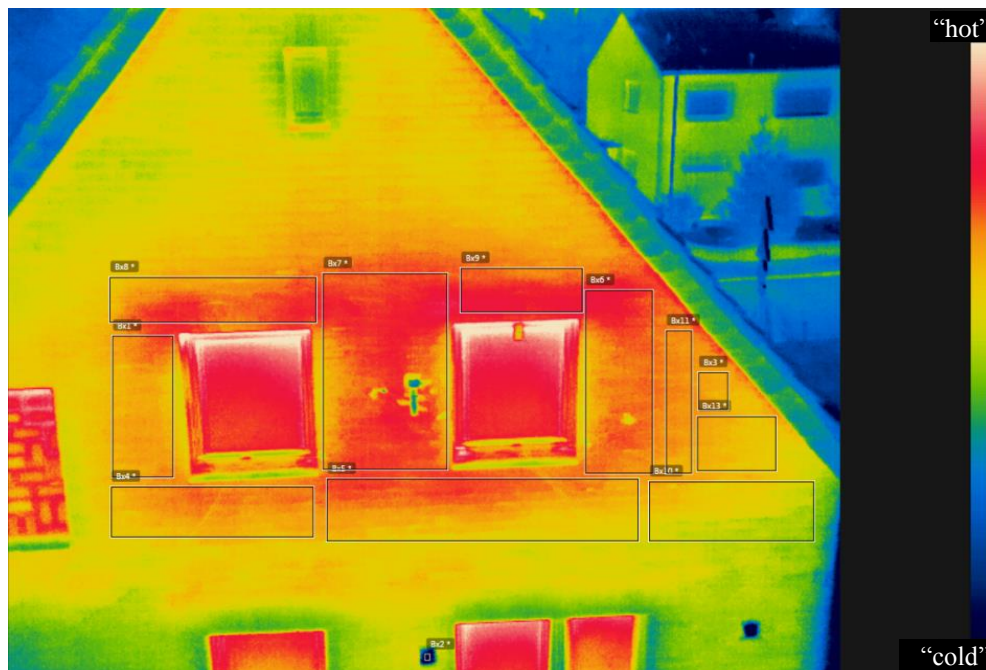


Figure 9: U-value calculation with multiple areas on the north wall

## 7. Data processing

After acquiring various kinds of remote sensing data, they have to be merged to form a base for energetic building simulation. For this purpose software to create object-oriented digital building models is being developed using the programming language Python. This section contains information about the concept of the modelling approach, the steps for the import of geometrical data, and the connection to building simulation tools.

### *Concept of modelling approach*

The output of photogrammetric building reconstruction is a CityGML file in level of detail (LoD) 3 containing information about the exterior surfaces of the structure and their semantic classification into walls, roofs, and

windows. The software design resembles the CityGML semantics: Surface objects are defined by exterior and interior polygons which in turn are declared by position objects as corner points. Neighboring surfaces share the respective position objects. For volumetric objects, the concept assigns every part of the building to one of the volumetric categories (e.g. room, window, wall, or roof). The respective objects share their bounding surfaces with their neighbors. As a consequence, the surfaces bounding only one volumetric part of a particular building define its outer hull. To the other sides of these surfaces there is ground, a part of another building, or empty space (air). When importing groups of buildings, the volumetric parts of adjacent structures can share bounding surfaces, making it possible to efficiently identify energetically important neighbor relations. Surface, volume and building objects are intended to get attributes that are useful for building analysis. Exemplary attributes are shown in Figure 10 which gives an overview of the object-oriented concept of the software.

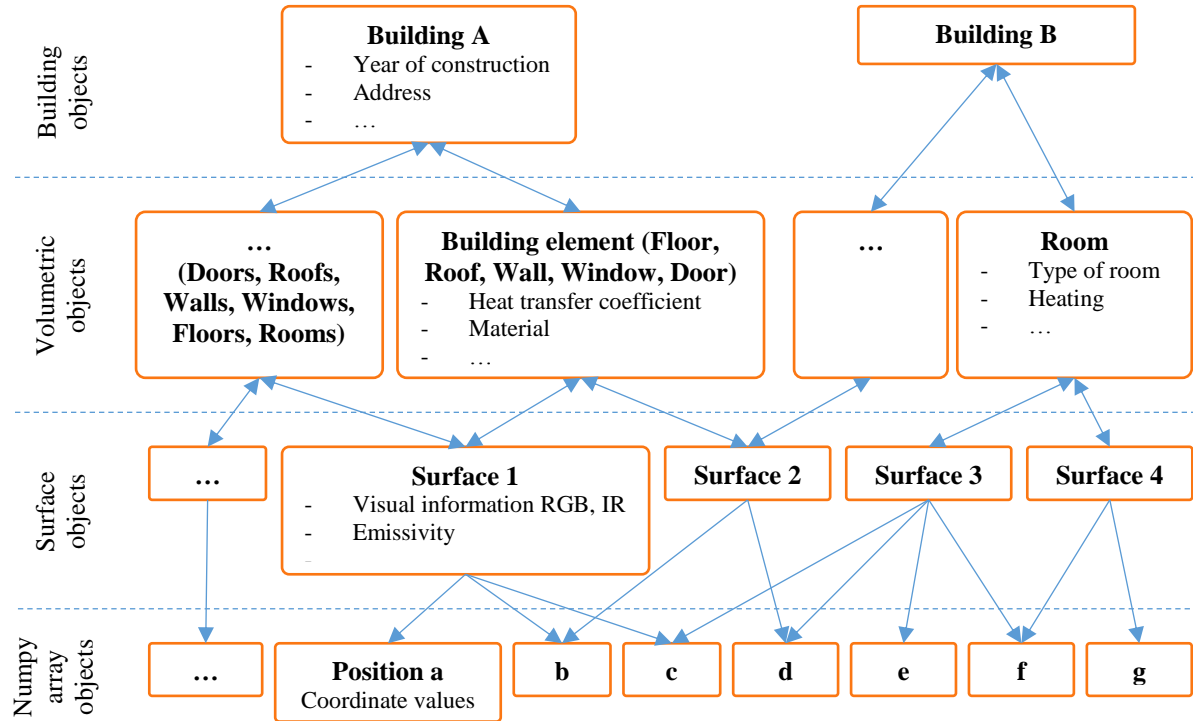


Figure 10: Concept for object-oriented modelling approach

*Pre-processing steps*

When reading CityGML LoD 3 files from the building reconstruction process presented in section 5, buildings are assembled from semantically annotated polygonal envelope surfaces. These surfaces are imported into the model as volumetric building elements with coplanar front and back surfaces. One room object per building is confined by the back surfaces of its envelope elements. During the import process, it is ensured that if equal coordinate values appear for different surfaces, the same position object is used.

With this information small irregularities in the planarity of the surfaces that occur due to the used reconstruction algorithm can be compensated. Coordinates that are part of perfectly planar surfaces are kept constant; the other wall and floor planes get vertically and horizontally aligned respectively while roof planes are fitted to the initial coordinates. Coordinates of corners are calculated as intersection points of the planes. As windows and doors are usually embedded into a surrounding surface, the positions defining them are usually set by the fitting of these surfaces.

The algorithm for introducing wall thicknesses and story-separating floors is currently under development. This includes the derivation of story heights (including the height of the lowest floor for the estimation of building elements below the ground) from the positions of windows, balconies, and/or story-separating ceilings visible in

thermal images. As back surfaces of walls interfere with other volumetric objects if they are extruded orthogonally to their front counterpart, changes to all adjacent objects must be conducted consistently and simultaneously. Another important issue in this context is the complexity of the relation between windows and walls which are coplanar surfaces in the CityGML file, but not in reality.

#### *Connection to building simulation tools*

One of the development goals of the modelling software is a flexible interface to building simulation software such as the generation of EnergyPlus input data files (idf), the connection to the Modelica Buildings library via the Python package `buildingspy` [21], or the simplification of building information to connect to tools like TEASER [22] for urban-scale simulation or BuildingOPT [23] for retrofit optimization. As data quality and availability vary between different buildings and input data requirements also vary between simulation tools, it is important to choose the best information available for the respective purpose and to include a possibility to complete necessary information with the help of other data sources like building typologies. In order to improve the quality of the simulation, all information that can be easily obtained by residents or owners should be included in the model, starting from the year of construction up to the age of the windows and their material and glazing type. Solar irradiation onto the building can be calculated using a polygon clipping algorithm on the 3D models.

## **8. Summary, conclusion, and outlook**

In this paper, measurement and data processing techniques for the energetic assessment of buildings were presented using a German single-family house as a reference building. Conventional tools for this purpose including laser scans, U-value detection from material information, U-value measurements, blower door tests, on-site inspections and general information sources were used in conjunction with commercially or openly available software tools to obtain a simulation model of the building that was afterwards validated against measured temperature and heating load data. The resulting data set provides reference values for a (hopefully) equivalent but more cost-efficient remote sensing approach as a part of the “building tomograph” project. Until now, a building reconstruction workflow based on close-range UAV photogrammetry in the visible spectrum and U-value quantification by infrared thermography has been tested on the reference building.

There is no significant indication for sensor-caused accuracy issues between laser scans and photogrammetrically generated point clouds. However, there are some differences in visibility of parts of the building that result from the positions the respective devices have been operated from and in how color information gets added. While photogrammetric point cloud generation nowadays can be quickly achieved with ready-to-use software tools, retrieving a semantically annotated and textured building hull will remain computationally expensive particularly if visibility tests on occluding objects are involved. Nevertheless, the inline approach used for “building tomograph” is nearly fully automatic and allows recognizing wall surface openings like windows.

Concerning U-value measurements, the proposed method hinged on quantitative infrared thermography is not yet able to compete with U-value calculation based on material information or the heat flux meter method. However, sufficient data on the material of the building wall is not generally available. Furthermore, the approach described is still under development and has the potential to reach a higher accuracy, especially when microwave radar and hyperspectral sensors will eventually be introduced.

Thus, future work will concentrate on the development and evaluation of new remote sensing technologies for wall material analyses and air leakage detection. Strategies remain to be developed and refined on how the data from additional sources can be fused and stored efficiently and consistently. This also includes the identification and definition of interfaces between measurement data collection and energetic building simulation software. To further increase the quality of the validation data set, a new measurement campaign is planned on the reference building. This will involve a pressure difference sensor, a weather station also recording soil temperature, continuous monitoring of the heat energy consumed, and coverage of the cooling phase of the building.

## 9. Acknowledgements

The authors gratefully acknowledge the German Ministry for Economic Affairs and Energy for funding this work in the framework of the “building tomograph” (Gtom) project (03ET1405A). Furthermore, the authors wish to thank RWE AG for providing access to the building in Morschenich that now serves as reference building.

## 10. References

- [1] S. Zundel and I. Stieß, “Beyond Profitability of Energy-Saving Measures—Attitudes Towards Energy Saving,” *J Consum Policy*, vol. 34, no. 1, pp. 91–105, 2011.
- [2] J. Estevam Schmiedt *et al.*, “Remote sensing techniques for building models and energy performance studies of buildings,” in *EBC Annex 71: Building energy performance assessment based on in-situ measurements: First expert meeting*, 2017.
- [3] G. N. Walton, U. States, N. B. o. Standards, D. o. Energy, and B. E. S. Branch, *Thermal analysis research program reference manual*. Washington, DC: U.S. Dept. of Commerce, National Bureau of Standards, 1983.
- [4] American society of heating refrigerating and air conditioning engineers, *2001 ASHRAE Handbook. Fundamentals*. Atlanta: ASHRAE, 2001.
- [5] E. M. Sparrow, J. W. Ramsey, and E. A. Mass, “Effect of Finite Width on Heat Transfer and Fluid Flow about an Inclined Rectangular Plate,” *J. Heat Transfer*, vol. 101, no. 2, p. 199, 1979.
- [6] X. Yin, P. Wonka, and A. Razdan, “Generating 3D Building Models from Architectural Drawings: A Survey,” *IEEE Comput. Graph. Appl.*, vol. 29, no. 1, pp. 20–30, 2009.
- [7] A. Sankar and S. Seitz, “Capturing indoor scenes with smartphones,” in *Proceedings of the 25th annual ACM symposium on User interface software and technology*, Cambridge, Massachusetts, USA, 2012, p. 403.
- [8] A. Haas, M. Peichl, and S. Dill, “Theoretical and experimental investigations of microwave signatures for characterization of building structures,” in *2017 18th International Radar Symposium (IRS)*, Prague, Czech Republic, 2017, pp. 1–10.
- [9] A. Haas, M. Peichl, and S. Dill, “Characterization of building structures with SAR,” in *Proceedings of EUSAR 2018: 12th European Conference on Synthetic Aperture Radar: 4-7 June 2018*, Aachen, 2018.
- [10] B. Kölsch, A. Tiddens, B. Schiricke, J. Estevam Schmiedt, and B. Hoffschmidt, “Detection of Air Leakage in Building Envelopes Using Ultrasound Technology,” in *Symposium on Whole Building Air Leakage: Testing and Building Performance*, San Diego, 2018 (under review).
- [11] M. Gilje, U. Heiden, M. Habermeyer, A. Mende, and C. Juergens, “Detecting Unknown Artificial Urban Surface Materials Based on Spectral Dissimilarity Analysis,” (eng), *Sensors (Basel, Switzerland)*, vol. 17, no. 8, 2017.
- [12] S. Mayer, “Automatisierte Objekterkennung zur Interpretation hochauflösender Bilddaten in der Erdfernerkundung,” Humboldt-Universität zu Berlin, Mathematisch-Naturwissenschaftliche Fakultät II, 2004.
- [13] D. Frommholz, M. Linkiewicz, H. Meissner, D. Dahlke, and A. Poznanska, “Extracting Semantically Annotated 3D Building Models with Textures from Oblique Aerial Imagery,” *Int. Arch. Photogramm. Remote Sens. Spatial Inf. Sci.*, vol. XL-3/W2, pp. 53–58, 2015.
- [14] D. Frommholz, M. Linkiewicz, and A. M. Poznanska, “Inlining 3D Reconstruction, Multi-source Texture Mapping and Semantic Analysis Using Oblique Aerial Imagery,” *Int. Arch. Photogramm. Remote Sens. Spatial Inf. Sci.*, vol. XLI-B3, pp. 605–612, 2016.
- [15] D. Frommholz, M. Linkiewicz, H. Meissner, and D. Dahlke, “Reconstructing Buildings with Discontinuities and Roof Overhangs from Oblique Aerial Imagery,” *Int. Arch. Photogramm. Remote Sens. Spatial Inf. Sci.*, vol. XLII-1/W1, pp. 465–471, 2017.
- [16] M. A. Fischler and R. C. Bolles, “Random sample consensus: A paradigm for model fitting with applications to image analysis and automated cartography,” *Commun. ACM*, vol. 24, no. 6, pp. 381–395, 1981.
- [17] P. A. Fokaides and S. A. Kalogirou, “Application of infrared thermography for the determination of the overall heat transfer coefficient (U-Value) in building envelopes,” *Applied Energy*, vol. 88, no. 12, pp. 4358–4365, 2011.
- [18] B. Tejedor, M. Casals, M. Gangolells, and X. Roca, “Quantitative internal infrared thermography for determining in-situ thermal behaviour of façades,” *Energy and Buildings*, vol. 151, pp. 187–197, 2017.

- [19] D. Patel, J. Estevam Schmiedt, M. Röger, and B. Hoffschmidt, “Approach for external measurements of the heat transfer coefficient (U-value) of building envelope components using UAV based infrared thermography,” in *14th Quantitative InfraRed Thermography Conference (QIRT)*, Berlin, 2018.
- [20] *ISO 9869-1 Thermal insulation\_building elements*, ISO 9869-1:2014(E), 2014.
- [21] M. Wetter, W. Zuo, T. S. Nouidui, and X. Pang, “Modelica Buildings library,” *Journal of Building Performance Simulation*, vol. 7, no. 4, pp. 253–270, 2014.
- [22] P. Remmen *et al.*, “TEASER: An open tool for urban energy modelling of building stocks,” *Journal of Building Performance Simulation*, pp. 1–15, 2017.
- [23] T. Schütz, L. Schiffer, H. Harb, M. Fuchs, and D. Müller, “Optimal design of energy conversion units and envelopes for residential building retrofits using a comprehensive MILP model,” *Applied Energy*, vol. 185, pp. 1–15, 2017.